

## Accepted Manuscript

Mimicking respiratory phosphorylation using purified enzymes

Christoph von Ballmoos, Olivier Biner, Tobias Nilsson, Peter Brzezinski

PII: S0005-2728(15)00252-2  
DOI: doi: [10.1016/j.bbabi.2015.12.007](https://doi.org/10.1016/j.bbabi.2015.12.007)  
Reference: BBABIO 47571

To appear in: *BBA - Bioenergetics*

Received date: 17 August 2015  
Revised date: 17 November 2015  
Accepted date: 16 December 2015



Please cite this article as: Christoph von Ballmoos, Olivier Biner, Tobias Nilsson, Peter Brzezinski, Mimicking respiratory phosphorylation using purified enzymes, *BBA - Bioenergetics* (2015), doi: [10.1016/j.bbabi.2015.12.007](https://doi.org/10.1016/j.bbabi.2015.12.007)

This is a PDF file of an unedited manuscript that has been accepted for publication. As a service to our customers we are providing this early version of the manuscript. The manuscript will undergo copyediting, typesetting, and review of the resulting proof before it is published in its final form. Please note that during the production process errors may be discovered which could affect the content, and all legal disclaimers that apply to the journal pertain.

## Mimicking respiratory phosphorylation using purified enzymes

Christoph von Ballmoos<sup>1#</sup>, Olivier Biner<sup>1\*</sup>, Tobias Nilsson<sup>2\*</sup> & Peter Brzezinski<sup>2</sup>

<sup>1</sup> Present address: Department of Chemistry and Biochemistry, University of Bern,  
Freiestrasse 3, 3012 Bern, Switzerland

<sup>2</sup> Department of Biochemistry and Biophysics, The Arrhenius Laboratories for Natural  
Sciences, Stockholm University, SE-106 91 Stockholm, Sweden.

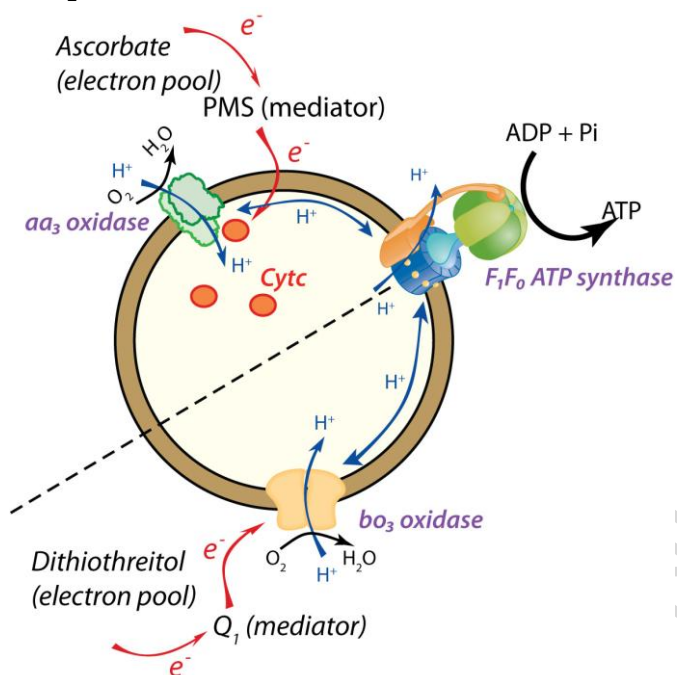
\* Contributed equally to the manuscript

# Correspondence: christoph.vonballmoos@dcb.unibe.ch

### Abstract

The enzymes of oxidative phosphorylation are a striking example of the functional association of multiple enzyme complexes, working together to form ATP from cellular reducing equivalents. These complexes, such as cytochrome *c* oxidase or the ATP synthase, are typically investigated individually and therefore, their functional interplay is not well understood. Here, we present methodology that allows the co-reconstitution of purified terminal oxidases and ATP synthases in synthetic liposomes. The enzymes are functionally coupled via proton translocation where upon addition of reducing equivalents the oxidase creates and maintains a transmembrane electrochemical proton gradient that energizes the synthesis of ATP by the F<sub>1</sub>F<sub>0</sub> ATP synthase. The method has been tested with the ATP synthases from *E. coli* and spinach chloroplasts, and with the quinol and cytochrome *c* oxidases from *E. coli* and *Rhodobacter sphaeroides*, respectively. Unlike in experiments with the ATP synthase reconstituted alone, the setup allows *in vitro* ATP synthesis under steady state conditions, with rates up to 90 ATP x s<sup>-1</sup> x enzyme<sup>-1</sup>. We have also used the novel system to study the phenomenon of “mild uncoupling” as observed in mitochondria upon addition of low concentrations of ionophores (e.g. FCCP, SF6847) and the recoupling effect of 6-ketocholestanol. While we could reproduce the described effects, our data with the *in vitro* system does not support the idea of a direct interaction between a mitochondrial protein and the uncoupling agents as proposed earlier.

## Graphical abstract



## Keywords

ATP synthesis; respiratory chain; liposomes; mild uncoupling; ionophore; lateral proton diffusion

## Abbreviations

FCCP, Carbonyl cyanide-*p*-trifluoromethoxyphen; CCCP, Carbonyl cyanide *m*-chlorophenyl hydrazone;  $Q_1$ , ubiquinone  $Q_1$ ; ACMA, 9-amino-6-chloro-2-methoxyacridine; kCh, 6-ketocholestanol; *cytc*, cytochrome *c* oxidase

## Introduction

Proton translocation across biological membranes plays a major role during energy conversion from carbon sources to the universal energy carrier ATP. The highly exergonic hydrolysis of ATP to ADP drives numerous reactions in living cells. According to Peter Mitchell's chemiosmotic theory, reducing equivalents that are accumulated as a result of cellular metabolism are converted into a transmembrane electrochemical proton gradient, which is subsequently utilized by the  $F_1F_0$  ATP synthase to generate ATP from ADP and inorganic phosphate. While the  $F_1F_0$  ATP synthase is found in almost all organisms and its basic mechanism is universally conserved, the enzymes generating the transmembrane electrochemical gradient vary greatly between species. For example, the halophilic archaeon *Halobacterium salinarium* employs the light-driven proton pump bacteriorhodopsin while phototrophic bacteria or plants use photosynthetic reaction centers to charge the membrane. Mitochondria or aerobic bacteria employ a series of  $H^+$ -pumping respiratory-chain complexes to charge the membrane for ATP synthesis in a process termed oxidative phosphorylation (for review, see [1-5]). One class of these respiratory complexes is the terminal oxidases, which catalyze the reduction of oxygen to water by quinol or cytochrome *c*, and use part of the free energy released in this reaction to pump protons across the membrane. Terminal oxidases are relatively well characterized and understood in structural and functional detail, however, far less is known about the molecular interplay between these enzymes and the ATP-synthase.

In an ideal system the membrane is impermeable to protons to ensure a tight coupling between these two reactions, minimizing energy loss during the conversion process. It has been suggested, however that a weak uncoupling activity in mitochondria could be desirable under resting state conditions, where reducing equivalents are high (high NADH) and ATP consumption is low [6]. Under these conditions, the mitochondrial membrane would hyperpolarize and free electron carriers and oxygen could react together to form reactive oxygen species. Membrane hyperpolarization and reactive oxygen species have been considered key factors in degenerative processes as aging and apoptosis [7-10]. While a protein-mediated uncoupling mechanism (UCP 1) in brown adipose tissue is well known to create heat during animal hibernation [11], the process might also have a more general role in all tissues for the reasons mentioned above. Regulation by fatty acids and thyroid hormones has been proposed, but the precise mechanism is unclear [8, 12-14]. In this matter, classical uncoupling agents like FCCP and SF6847 at low concentrations have been shown to produce a similar effect that generally is termed "mild uncoupling". Under these conditions, the low dosages of uncoupling agents are sufficient to stimulate respiration (through a proton leak) without the complete abolishment of ATP synthesis activity.

To investigate the questions discussed above, either whole organelles (mitochondria, chloroplasts) or inverted membrane vesicles from bacteria were employed to study coupled enzyme function. While these systems have advantages (correct enzyme orientation, high density protein content), they share the common drawback of not being fully characterized or controllable. For example, many other enzymes are present in these membranes that are also sensitive to the electrochemical proton gradient, the lipid composition of the membrane cannot be controlled and analysis of mutant variants in more than one enzyme type is cumbersome. Very few examples of co-reconstituted isolated respiratory enzymes and ATP synthases are known. A notable exception is the co-reconstitution of an ATP synthase and the archaeal light-driven proton pump bacteriorhodopsin. The experiment was pioneered by Racker and Stoeckenius in 1974 with bacteriorhodopsin and a fraction of the mitochondrial membrane [15] and was crucial for the general acceptance of Mitchells chemiosmotic theory. The system was revived in the mid 90-ies by Rigaud and colleagues with the purified ATP synthase from a thermophilic bacillus PS3, performing extensive investigations on reconstitution conditions and energy requirements for ATP synthesis [16, 17]. In all these experiments, however, ATP synthesis rates were rather low, usually  $<5 \text{ ATP} \times \text{s}^{-1} \times \text{enzyme}^{-1}$ , which is far below those measured with whole organelles (e.g.  $>180 \text{ ATP} \times \text{s}^{-1} \times \text{enzyme}^{-1}$  for the ATP synthase of *Escherichia coli*) [18].

Here, we present the successful co-reconstitution of purified terminal oxidases from *E. coli* ( $bo_3$ ) and *Rhodobacter sphaeroides* ( $aa_3$ ) with the purified ATP synthases from *E. coli* or spinach chloroplasts. After addition of an electron source to initiate proton pumping by the oxidase, ATP synthesis was observed at rates up to  $90 \text{ ATP} \times \text{s}^{-1} \times \text{enzyme}^{-1}$  and can be driven under steady-state conditions as long electrons and  $\text{O}_2$  are available. We describe the relevant parameters of the setup and utilize it to investigate the impact of mitochondrial uncoupling agents on this minimal system mimicking oxidative phosphorylation.

## Materials and Methods

### Chemicals

Bovine cytochrome *c* and general chemicals were purchased from Sigma-Aldrich, if not otherwise indicated. CCCP and FCCP were from Santa Cruz Biotechnology. SF6847, valinomycin, nigericin and 6-ketocholestanol were purchased from Sigma-Aldrich. All inhibitors were dissolved in anhydrous EtOH. The luciferin-luciferase assay (CLS II) was purchased from Roche-Chemicals. Soybean lipids, Type II-S and 95% PC content were purchased from Sigma-Aldrich and Avanti Polar Lipids, respectively.

### **Purification of membrane proteins**

The *E. coli* ATP synthase containing a His-tag at the  $\beta$ -subunit was purified as described [19]. Purification of ATP synthase from spinach chloroplasts was performed as described [20]. The *E. coli*  $bo_3$  quinol oxidase was expressed with plasmid pETcyo, containing the sequence for oxidase subunit I-IV, with a His-tag at the C-terminus of subunit II, in strain BL21 ( $\Delta$ cyoABCDE) in LB medium, and induced with 0.5 mM IPTG, when the culture reached  $OD_{600}=0.5-0.6$  [21]. The  $aa_3$  oxidase from *R. sphaeroides* was purified as described [22]. For all protein preparations, droplets of the purified enzyme ( $\sim 30 \mu\text{l}$ ) were snap frozen in liquid nitrogen and stored at  $-80^\circ\text{C}$  to avoid repeated freeze-thaw cycles.

### **Liposome preparation**

Soybean lipids (95% PC) (10 mg/ml) were extensively re-suspended under nitrogen atmosphere in a buffer composed of 20 mM HEPES, pH 7.5, 2.5 mM  $\text{MgCl}_2$ , 25 g/l sucrose (buffer A) by vortexing until they appeared as a homogeneous suspension. Subsequently, the lipids were frozen in  $\text{LN}_2$  and thawed in water ( $30^\circ\text{C}$ ) and vortexed for 10 s. This procedure was repeated 5 times, yielding unilamellar liposomes. The suspension was then extruded using a pore diameter of 200 nm to obtain a homogeneous liposome preparation. As an alternative to the freeze/thaw procedure, subsequent extrusion procedures with 800 nm and 200 nm membranes were performed, yielding similar results.

### **Co-reconstitution of ATP synthase and terminal oxidase**

Typically, an amount of 480  $\mu\text{l}$  liposome suspension (10 mg/ml) was mixed with 15  $\mu\text{l}$  Na-cholate (from a 20% stock solution, final  $\sim 0.6\%$ ) to destabilize the liposomes. Proteins were added at desired concentrations from stock solutions and the mixture was incubated for 30 min at room temperature with occasional gentle shaking. The mixture was then applied to a prepacked Sepharose G-25 column (PD-10, GE Healthcare) equilibrated with 25 ml buffer A (see above). Subsequently, 2.4 ml buffer A were added, before the liposomes were collected with a final addition of 1.3 ml buffer A. If not otherwise stated, the obtained proteoliposomes were used directly.

### **Determination of phosphate concentration**

Phosphate concentration measurements in liposome suspensions were performed as described [23]. A standard curve was prepared for every set of measurements using a standardized phosphate solution (Sigma).

### **Determination of liposome size distribution**

The size distribution of liposome samples before and after reconstitution was assayed by Tunable Resistive Pulse Sensing (TRPS) with a qNano device (Izon Science, UK). Liposome samples were

diluted into measurement buffer (20 mM Hepes, 50 mM KCl) and applied on top of a stretchable pore (NP200) and traces with at least 1000 particles were recorded and averaged. Calibration was performed with carboxylated polystyrene beads (200 nm). Data analysis was performed with the IZON Control Suite (IZON Science).

### **Proton-uptake measurements with ACMA**

Sixty  $\mu\text{l}$  of proteoliposomes were diluted into 1.5 ml of a buffer composed of 20 mM Hepes-KOH, pH 7.5, 5 mM  $\text{MgCl}_2$ , 100 mM KCl (HMK buffer), mixed with 2  $\mu\text{M}$  9-Amino-6-Chloro-2-Methoxyacridine (ACMA) and stirred in a 5 ml fluorescence cuvette until a stable baseline was obtained. Proton pumping was initiated by the addition of 2 mM Na-ATP for the ATP synthase or 2 mM DTT/20  $\mu\text{M}$  ubiquinol  $\text{Q}_1$  for the  $\text{bo}_3$  oxidase. After the reaction had reached an equilibrium, the proton gradient was dissipated upon addition of 10 mM  $\text{NH}_4\text{Cl}$ . Changes in the fluorescence signals were monitored on a Cary Eclipse, using 410 nm and 480 nm as excitation and emission wavelengths, respectively. The slits were set at 5 nm.

### **ATP synthesis measurements**

Typically, 20  $\mu\text{l}$  of proteoliposomes were added to 470  $\mu\text{l}$  of a buffer composed of 20 mM Tris- $\text{PO}_4$ , pH 7.5, 5 mM  $\text{MgCl}_2$ , and supplemented with 0.8 mM ADP (2  $\mu\text{l}$  from a 20 mM stock solution) and 15  $\mu\text{l}$  CLS II luciferase/luciferin solution (10 mg/ml of powder in ddH<sub>2</sub>O). If the proteoliposomes contained  $\text{bo}_3$  oxidase, 2 mM DTT (from 1M stock) was added before recording a baseline on a Glomax luminometer (Promega). Time spans of 30 s with a data point every second were measured between different additions. First, 20  $\mu\text{M}$  ubiquinol  $\text{Q}_1$  (1  $\mu\text{l}$  from 10 mM stock solution in EtOH) was added to initiate the reaction and ATP synthesis was followed. Three times 30 s were measured and the average slope of these three measurements was used as the rate. Further additions like inhibitor or ionophores were always added after the native measurement to minimize variation due to pipetting errors.

Standard curves were recorded for every measurement session by addition of discrete amounts of a 10  $\mu\text{M}$  ATP stock solution to a proteoliposome preparation as described above before the addition of the electron/mediator couple.

### **Steady-state activity of cytochrome *c* oxidase**

Steady-state activity was monitored by recording oxygen consumption using a Clark-type electrode (Hansatech Oxytherm) at room temperature. The starting solution contained 20 mM Hepes-KOH (pH 7.5), 0.05% DDM, 4 mM ascorbate, 0.5 mM N,N,N',N'-tetramethyl-p-phenylenediamine (TMPD), and 20  $\mu\text{M}$  bovine cytochrome *c*. The signal was allowed to stabilize before the reaction was started by the addition of 5 nM  $\text{aa}_3$  cytochrome *c* oxidase.

## Results

### Co-reconstitution of ATP synthase and $bo_3$ oxidase from *E. coli* into soybean liposomes

The method used for co-reconstitution was originally described by Rigaud and colleagues, and it was later adapted by Ishmukametov *et al.* for the ATP synthase from *E. coli* [24, 25]. It assumes formation of a ternary complex of liposomes, detergent molecules and the solubilized protein. Upon removal of the detergent, the membrane protein(s) integrate into the liposomal membrane. We have simplified this procedure for different ATP synthases by using disposable desalting columns, yielding uniformly oriented proteoliposomes, with the large  $F_1$  part being on the outside of the liposomes [19, 26]. The reconstitution efficiency for the ATP synthase and the  $bo_3$  oxidase was in our hands ~50%, when proteoliposomes were first clarified from aggregates by low spin centrifugation and then collected by ultracentrifugation [27]. We have also used the same procedure to incorporate cytochrome *c* oxidases from *Rhodobacter sphaeroides* ( $aa_3$ ) and *Thermus thermophilus* ( $ba_3$ ) with an orientation of 60% to 80% of the oxidases with the cytochrome *c* binding site facing the outside of the liposomes [28].

Since both ATP synthase and  $bo_3$  oxidase can be reconstituted using this method, we used the same approach to co-reconstitute them together into the same liposomal membrane (**Figure 1a**). Purified  $bo_3$  oxidase and ATP synthase (both from *E. coli*) were mixed and incorporated into liposomes at a 1:1 ratio aiming for ~10 enzymes (assuming 100 % reconstitution efficiency) of each type per liposome (**Figure 1a**). In order to estimate the liposome concentration, we have determined the phosphate concentration in samples before and after reconstitution (Supplementary table 1). From there, the number of lipids per liposome was calculated assuming a globular shape of the liposomes, a bilayer thickness of 5 nm and lipid area size of  $0.7 \text{ nm}^2$  [29]. The size of the liposomes before and after reconstitution was determined by tunable resistive pulse sensing and yielded liposomes close to the expected 200 nm that were used during liposome extrusion. The average size of the liposomes did not change during reconstitution, but liposomes containing proteins showed a broader distribution (Supplementary Figure 1 and Supplementary Table 1).

First, we verified the functional incorporation of both enzymes individually by testing their capability to induce transmembrane proton pumping. For the ATP synthase, this is typically done by measuring the acidification of the liposome inner volume upon addition of ATP (the  $F_1$  headpiece is on the outside [26], i.e. protons are pumped into the vesicles upon addition of ATP), monitored using the pH-sensitive dye ACMA (**Figure 1b**, red trace). Analogously, we measured the  $bo_3$  pumping activity after addition of the artificial electron donor DTT and water-soluble mediator ubiquinone  $Q_1$  (black trace). When both enzymes were energized simultaneously (green trace), an increased pumping



activity was observed, supporting co-reconstitution of the two different enzymes in the same membrane.

The proteoliposomes also reduced oxygen as measured using a Clark electrode. However, no significant respiratory-control ratio (RCR) was obtained upon addition of the  $K^+$  ionophore valinomycin and the protonophore CCCP (data not shown).

ACCEPTED MANUSCRIPT

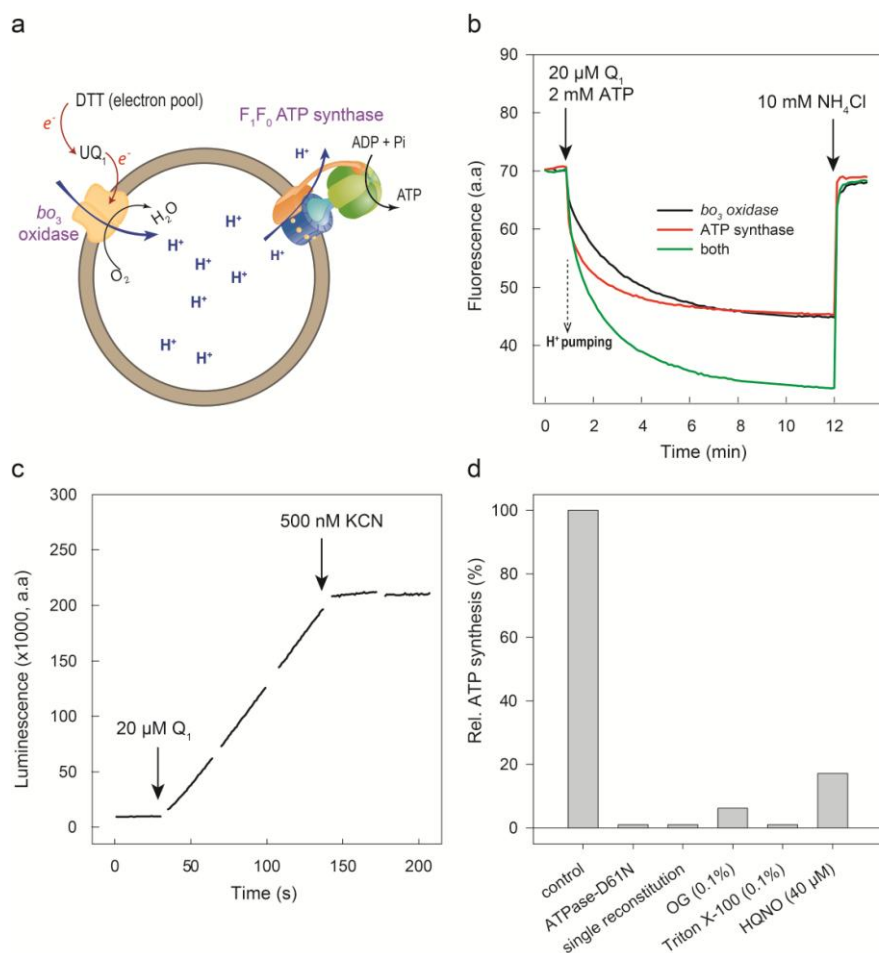


**Figure 1:** Respiratory-driven ATP synthesis employing  $bo_3$  oxidase and ATP synthase, both from *E. coli*.

(a) Cartoon showing proteoliposomes containing co-reconstituted ATP synthase and  $bo_3$  oxidase. The electron donor (DTT) and electron mediator (ubiquinol  $Q_1$ ) are also indicated. Shown is the proton flux during ATP synthesis with correctly oriented enzymes (b) ACMA fluorescence quenching experiments to monitor ATP synthase and  $bo_3$  oxidase proton pumping activity. In a 5 ml cuvette, 1.5 ml ACMA buffer (20 mM HEPES, pH 7.5, 5 mM  $MgCl_2$ ), 60  $\mu$ l proteoliposomes (containing  $bo_3$  oxidase and ATP synthase) and 2  $\mu$ M 9-Amino-6-Chloro-2-Methoxyacridine (ACMA) were mixed by stirring until a stable baseline was obtained. Proton pumping by the ATP synthase (red trace) or the  $bo_3$  oxidase (black trace) was initiated by the addition (left arrow) of 2 mM ATP or 4 mM DTT/20  $\mu$ M ubiquinol  $Q_1$ , respectively. Simultaneous proton pumping of the two enzymes is also shown (green trace). Addition of 10 mM  $NH_4Cl$  (right arrow) from a 1M stock solution dissipated the proton gradient. (c) Continuous respiratory-driven ATP synthesis was followed by measuring the luminescence using the luciferin/luciferase system detecting newly synthesized ATP. Indicated is the start of proton pumping upon addition of 20  $\mu$ M  $Q_1$  (left arrow) and inhibition of the oxidase upon addition of 0.5 mM potassium cyanide (right arrow). (d) Respiratory-driven ATP synthesis using the described protocol (control) was compared to preparations where either an inactive mutant variant of the ATP synthase (ATPase-D61N) was used or where the two enzymes were separately reconstituted into different vesicle preparations, which were then mixed prior to measurement (single reconstitution). Shown are also the effects of addition of detergents ( $\beta$ -octyl glucoside (OG) and Triton X-100 below and above the CMC, respectively) and a quinol oxidase inhibitor (HQNO). Experiments have been performed twice with two different enzyme preparations and the results from one experiment are shown.

### Respiratory-driven ATP synthesis

Because ATP synthase almost exclusively orients in an inside-out orientation with the  $F_1$  headpiece towards the outside [26], the respiratory oxidase has to pump protons to the inside of the liposomes (creating an inside positive and acidic electrochemical potential) for ATP synthesis to occur (see **Figure 1a**). As seen in Figure 1B, a net proton influx can be observed upon addition of DTT/ $Q_1$ , indicating the presence of proteoliposomes with a majority of correctly oriented  $bo_3$  oxidases that will energize ATP synthesis and create a luciferase signal.

*In situ* ATP synthesis was continuously followed using an ATP-sensitive luciferase/luciferin assay. The proteoliposomes were mixed with buffer containing  $Mg^{2+}$ , ADP, DTT, phosphate, luciferase/luciferin and a luminescence baseline was recorded, before the electron mediator ubiquinol  $Q_1$  was added to initiate proton pumping. As seen in **Figure 1c**, a linear increase in the luminescence signal was observed, indicating the continuous synthesis of ATP. Such a continuous production of ATP with a constant rate over several minutes is not observed in experiments in which the ATP synthase alone is reconstituted in vesicles because the proton-motive force (created by changing the pH on the outside of vesicles) is rapidly depleted, which leads to a decay of the synthesis rate after a few seconds [30, 31]. In our experiment with co-reconstituted  $bo_3$  oxidase however, a steady ATP production was observed as long as reductant and oxygen were present. ATP synthesis was completely abolished upon addition of the  $bo_3$  oxidase inhibitor potassium cyanide (Figure 1c).

The lipids used in these initial experiments were soybean asolectin lipids (Type II-S, ~14-20% PC content) that are widely used in reconstitution experiments. However, we found 4 times higher ATP synthesis rates when lipids with a higher PC content (95%) were used (Supplementary Table 1). The remainder of the experiments were thus performed with the 95% PC lipid source. A detailed influence of the lipid composition on respiratory-driven ATP synthesis will be described elsewhere. Care was taken that enough luciferin/luciferase was present during the measurement to ensure a linear relationship between luminescence signal and ATP concentration (Supplementary Figure 2).

### Control experiments and titration of important parameters

The optimal amount of cholate used in the reconstitution procedure was found to be around 0.6% when the lipid concentration was 10 mg/ml (Supplementary Figure 3). Slightly lower (0.4%) and higher (1%) cholate concentrations were found to be optimal with lipid concentrations of 5 mg/ml and 20 mg/ml, respectively (data not shown).

Next, we tested the behavior of the co-reconstituted proteoliposomes in a variety of experimental conditions (**Figure 1d**). As expected, no ATP synthesis was detected when the enzymes were reconstituted separately into different liposomes, which were then mixed or when an inactive

mutant of the ATP synthase was used (D61N in subunit c lacks the proton binding site on the c-ring). Inhibition of the terminal oxidases ( $bo_3$  and  $aa_3$ ) was achieved by addition of potassium cyanide, which also inhibited ATP synthesis. Addition of HQNO, an inhibitor of the quinol oxidase, decreased ATP synthesis to 15% of that measured before HQNO addition, comparable to the reduction found in oxygen consumption measurements with the  $bo_3$  oxidase (~20%, data not shown). Addition of  $\beta$ -octylglucoside below its critical micellar concentrations (CMC) led to a strongly decreased ATP synthesis rate, while addition of Triton X-100 above its CMC completely abolished synthesis. These results show that respiratory driven ATP synthase is only possible in proteoliposomes with an intact membrane containing both enzymes.

We also titrated the various components (inorganic phosphate, DTT, ubiquinol  $Q_1$  and ADP) required for ATP synthesis. One component was varied at the time, while the others were present at excess concentrations (**Figure 2a-d**). The apparent  $K_m$  values were for DTT ~116  $\mu$ M, ADP ~4  $\mu$ M, phosphate ~1.2 mM and  $Q_1$  ~5  $\mu$ M. The values found for ADP and phosphate were in the same order as those reported previously for the isolated ATP synthase in liposomes (~27  $\mu$ M and ~0.9 mM, respectively) [30], but somewhat different from those found for the bacteriorhodopsin/ATP synthase system (ADP ~300  $\mu$ M, 10 mM ~phosphate) [32]. However, in the latter case, ATP synthase from the thermophilic bacterium PS3 was used and measurements were performed at 40°C, which could account for the different apparent affinities.

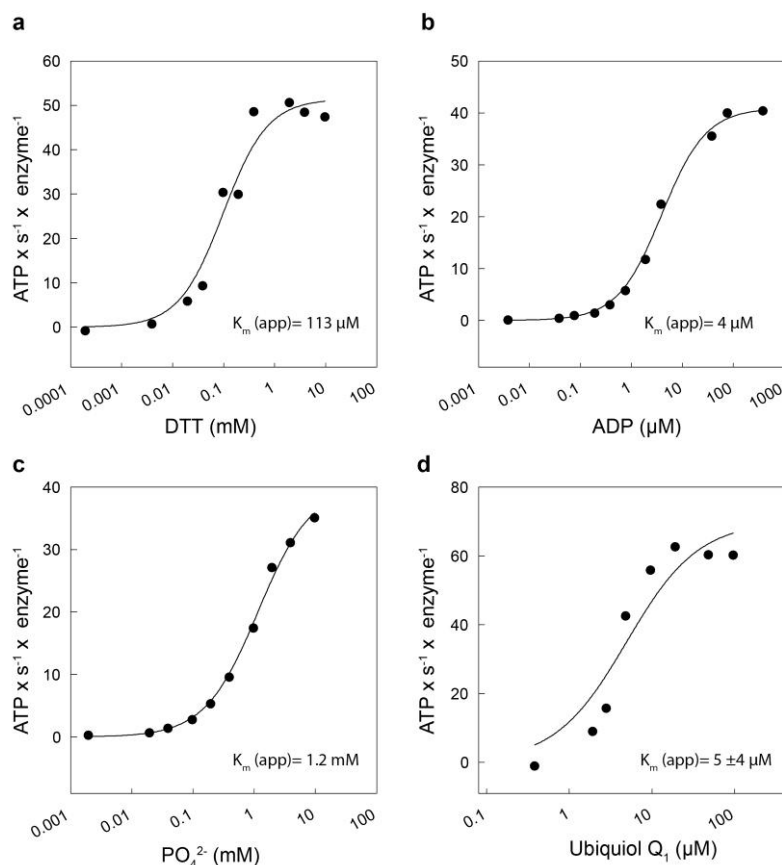


**Figure 2:** Titrations of different components required for respiratory ATP synthesis.

(a) DTT was added to a proteoliposome suspension containing 20 mM phosphate, 20 μM ubiquinol Q<sub>1</sub> and 80 μM ADP and the averaged ATP-synthesis rate after 90 s was determined. (b) Same as in (a), but ADP at different concentrations was added to a proteoliposome suspension containing 20 mM phosphate, 20 μM ubiquinol Q<sub>1</sub> and 4 mM DTT. (c) Same as in (a), but phosphate at different concentrations (from a pH-adjusted Na-phosphate stock) was added to a proteoliposome suspension containing 4 mM DTT, 80 μM ADP and 20 μM ubiquinol Q<sub>1</sub>. (d) Same as in (a), but ubiquinol Q<sub>1</sub> at different concentrations was added to a proteoliposome suspension containing 20 mM phosphate, 4 mM DTT and 80 μM ADP. Shown are the data together with a fit for a single binding site. The apparent K<sub>m</sub> values are given. The K<sub>m</sub> values were averaged from two (DTT, phosphate, ADP) or three (ubiquinol Q<sub>1</sub>) measurements with different liposome preparations. Error bars in a, b and c are omitted, because only two measurements with very similar results were performed.

### Effect of uncouplers and ionophores on respiratory-driven ATP synthesis

Small molecules like  $\text{NH}_4\text{Cl}$ , Nigericin, CCCP, FCCP and SF6847, the three latter also known as mitochondrial uncoupling agents, are known to dissipate the proton gradient across a membrane. Addition of these molecules was shown to impair ATP synthesis in earlier *in vitro* measurements [30, 31], in which a valinomycin/potassium diffusion gradient was used to create a transient membrane potential. We took advantage of our system with a continuously maintained driving force and tested the effects of commonly used uncoupling reagents and the ionophore valinomycin. First, we tested the effect of  $\text{NH}_4\text{Cl}$  that dissipates the chemical proton gradient, while the electrical gradient is unaffected. Formation of a pH gradient and ATP synthesis in the presence or absence of  $\text{NH}_4\text{Cl}$  was followed by ACMA fluorescence and luciferase measurements, respectively (**Figure 3a**). While no ACMA-quenching signal was detected upon initiation of proton pumping in the presence of  $\text{NH}_4\text{Cl}$  (**Figure 3, red trace**), the ATP synthesis rate under the same conditions was only marginally affected (**Figure 3a, inset**). In other words, the ACMA data show that while no chemical proton gradient was formed, synthesis of ATP was still possible with the remaining driving forces present (see discussion).

Next, the influence of the  $\text{K}^+$  ionophore valinomycin on the respiratory-driven ATP synthesis was tested (with 50 mM KCl on both sides of the liposomes). In the presence of potassium, valinomycin dissipates the electrical potential by selective transport of charged  $\text{K}^+$  species, while the chemical proton gradient is not affected. No substantial loss in ATP synthesis was observed up to a final concentrations of 2  $\mu\text{M}$  valinomycin (**Figure 3b**). When used together with the electroneutral proton-potassium antiporter nigericin, much smaller amounts of valinomycin (200 nM) and nigericin (500 nM) were sufficient to completely inhibit ATP synthesis. Nigericin alone had only a negligible influence on ATP synthesis at the tested concentrations (up to 500 nM). The combination of valinomycin and  $\text{NH}_4\text{Cl}$  did also completely abolish ATP synthesis (data not shown). Taken together, this data indicates that ATP synthesis is only abolished when both components of the driving force are dissipated at the same time.

The influence of the widely used protonophore and mitochondrial uncoupling agent FCCP was also investigated. ATP synthesis decreased with increasing FCCP concentrations, with a remaining activity of about  $45 \pm 20\%$  at 100 nM final FCCP concentration. Addition of 500 nM valinomycin further suppressed ATP synthesis to 10% (**Figure 3b**). The uncoupling mechanism of FCCP is more complex, it affects both the proton gradient and the membrane potential simultaneously [33]. After neutral FCCP has released the proton, the negative charge is distributed in a conjugated aromatic ring system allowing the anionic form of FCCP to freely diffuse in the membrane. In other words, FCCP combines the effects of nigericin or  $\text{NH}_4\text{Cl}$  with that of valinomycin and therefore typically acts at lower concentrations.

It has been found that the effect of FCCP and other uncoupling agents at mild uncoupling conditions in mitochondria (see Introduction) could be reversed by the addition of 6-ketocholestanol (kChe) [34, 35]. It was speculated that at low concentrations, the uncoupling agents bind to cytochrome *c* oxidase (or another mitochondrial protein) and that this binding would be impeded in the presence of 6-ketocholestanol that accumulates in the outer leaflet of the membrane [34]. All these measurements have been performed by following either oxygen consumption or the presence of a membrane potential, but the effect of 6-ketocholestanol on ATP synthesis has not been directly tested. We therefore investigated the influence of 6-ketocholestanol with our co-reconstituted system containing a *bo*<sub>3</sub> oxidase and ATP synthase. As seen in **Figure 3c**, in the presence of 50 nM FCCP, ATP synthesis dropped to ~50%, but was recovered to 80% after addition of 25  $\mu$ M 6-ketocholestanole. The recovery was also observed with low concentrations of CCCP and SF6847. In the latter case, recovery to almost 100% was most impressive, exactly reproducing the data from mitochondrial experiments [35]. Addition of the same amount of cholesterol did not show any recovering effect (data not shown). ATP synthesis activity was also partly recovered by 6-ketocholestanole in the presence of both SF6847 and valinomycin, indicating that it slows the overall uncoupling process (Figure 3c, last column).

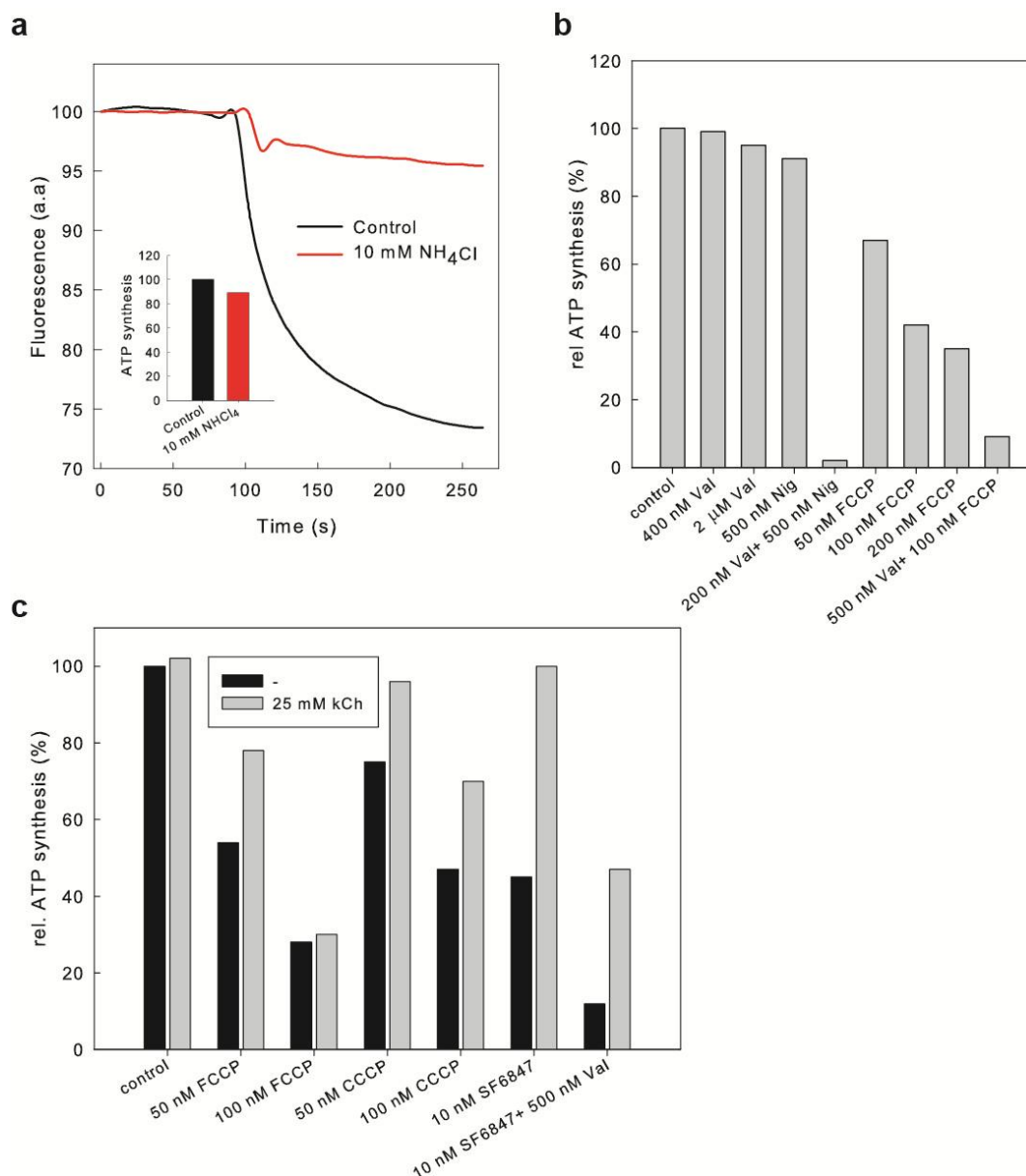


**Figure 3:** Effect of uncouplers, ionophores and 6-ketocholestanol on respiratory-driven ATP synthesis.

(a) In a 5 ml cuvette, 1.5 ml ACMA buffer (20 mM HEPES, pH 7.5, 5 mM MgCl<sub>2</sub>), 60 μl proteoliposomes (containing *bo*<sub>3</sub> oxidase and ATP synthase), 2 μM ACMA and 4 mM DTT were mixed by continuous stirring, before 20 μM ubiquinol Q<sub>1</sub> was added, either in the absence (black trace) or presence (red trace) of 10 mM NH<sub>4</sub>Cl. Respiratory driven ATP synthesis with the same proteoliposomes in the same buffers is shown as an inset. (b) Effect of various uncouplers on respiratory-driven ATP synthesis using proteoliposomes containing *bo*<sub>3</sub> oxidase and ATP synthase. First, the rate over 60 s was measured. Then, the rate was measured again over 60 s after addition of the indicated compound. The effects are presented as the relative ratio of the two rates. Shown are averaged values obtained with two proteoliposome preparations measured in duplicates. (c) Effect of 6-ketocholestanol on the ATP-synthesis activity in the presence of low concentrations of uncoupling agents. First, the rates before and after the addition of the uncoupler were determined. Then, 25 μM 6-ketocholestanol was added and the rate was again measured. The effects are represented as the ratio of the uncoupled/recoupled rate and the rate before addition of any compound rates. Shown are the results from a typical set of measurements. The experiment was performed with three sets of proteoliposomes with similar results.



**Reconstitution of respiratory enzymes from other organisms than *E. coli***

The protocol described above was also tested for co-reconstitution of respiratory enzymes from other organisms than *E. coli*. The ATP synthase from spinach chloroplasts was purified according to the protocols developed by Turina *et al.* [20] and used together with the  $bo_3$  oxidase from *E. coli*. ATP synthase prepared using this method is less pure and an accurate estimate of the concentration (by a BCA protein concentration assay) is difficult. The ATP synthesis rate with the chloroplast ATP-synthase was about 70% of that obtained with the *E.coli* ATP-synthase, which is well within the accuracy of the protein concentration determination (data not shown).

While quinol-type oxidases such as the  $bo_3$  from *E. coli* are only found in bacteria, the prevailing type of terminal oxidases in respiring organisms, characterized to date, is the A-type cytochrome *c* oxidase found in many bacteria and mitochondria [36, 37]. In this class of enzymes, electrons are donated to the oxidase by cytochrome *c*, which in the living cell receives electrons from the  $bc_1$  complex. Cytochrome *c* is found in the bacterial periplasm or the inter-membrane space of mitochondria, i.e. on the opposite side of the membrane to that where ATP synthesis occurs. Therefore, in our liposome experiments, in the fraction of oxidases that are oriented such that they could pump protons to the inside, the cytochrome *c* binding site is located on the inside of the liposomes. As we have to add the electron source to the outside of the liposomes, an electron donor/mediator couple was used that is capable to transport the electrons across the membrane (**Figure 4a**). Out of the many combinations of reductant/mediator tested, ascorbate (2 mM) and phenazine methosulfate (PMS, 10  $\mu$ M) was found to be the most effective couple. In these experiments, we also included soluble cytochrome *c* at various concentrations (to ensure efficient electron transport to the cytochrome *c* oxidase) in our reconstitution mixture prior to detergent removal. As the non-incorporated cytochrome *c* (12 kDa) co-elutes with the liposomes during gel filtration (PD-10 has a cutoff of  $\sim$ 5 kDa), the suspension was passed through a weak cation exchange resin (pI of cytochrome *c* is about 9.5) to which external cytochrome *c* was adsorbed.

In the presence of increasing cytochrome *c* concentrations, increasing ATP synthesis rates were observed with an apparent  $K_m$  of  $\sim$ 11  $\mu$ M, based on the cytochrome *c* concentration in the reconstitution mixture (**Figure 4b**). In the absence of cyt *c*, the rates were  $\sim$ 20%, caused by direct reduction of cytochrome *c* oxidase by PMS. The maximal measured ATP synthase rates were in the same range as those found with the  $bo_3$  oxidase when similar amounts of enzyme were employed in reconstitution, indicating that the two oxidases are similarly efficient in producing and maintaining a transmembrane electrochemical proton gradient. We also performed experiments with a selection of ionophores, analogously to the system with the  $bo_3$  oxidase as described above (**Figure 4c**). Qualitatively, we observed the same effects, but inhibition by FCCP was observed at already lower

concentrations ( $IC_{50} \sim 15$  nM ( $\alpha\alpha_3$ ) vs  $\sim 75$  nM ( $bo_3$ ) (Supplementary Figure 4). Using different amounts of PMS, we found that the apparent  $IC_{50}$  of FCCP is dependent on the concentration of PMS, explaining the reduced  $IC_{50}$  values found (data not shown). We speculate that in addition to its electron mediating function, PMS does also dissipate the membrane potential when the positively charged (oxidized) form is transported across the membrane along the electrical gradient, thus imitating the effect of valinomycin (see discussion). Analogously to the experiment with  $bo_3$  oxidase, uncoupling by SF6748 was almost fully recovered by addition of 6-ketocholestanol, suggesting that this process is independent of the enzyme used (**Figure 4c**).

We also measured respiratory-driven ATP synthesis with a structural variant of cytochrome *c* oxidase, which has been shown earlier to be highly active in oxygen turnover ( $\sim 150$  % of that with the wild type cytochrome *c* oxidase), but is unable to pump protons across the membrane (the replacement N139D was introduced in subunit I [38]). A similar ATP synthesis rate to that observed with the wild type enzyme was found when similar amounts of oxidase were used in reconstitution (**Figure 4d**). No activity was found with the D132A variant in which the turnover rate is  $< 5$  % of that in the wild-type oxidase [39].

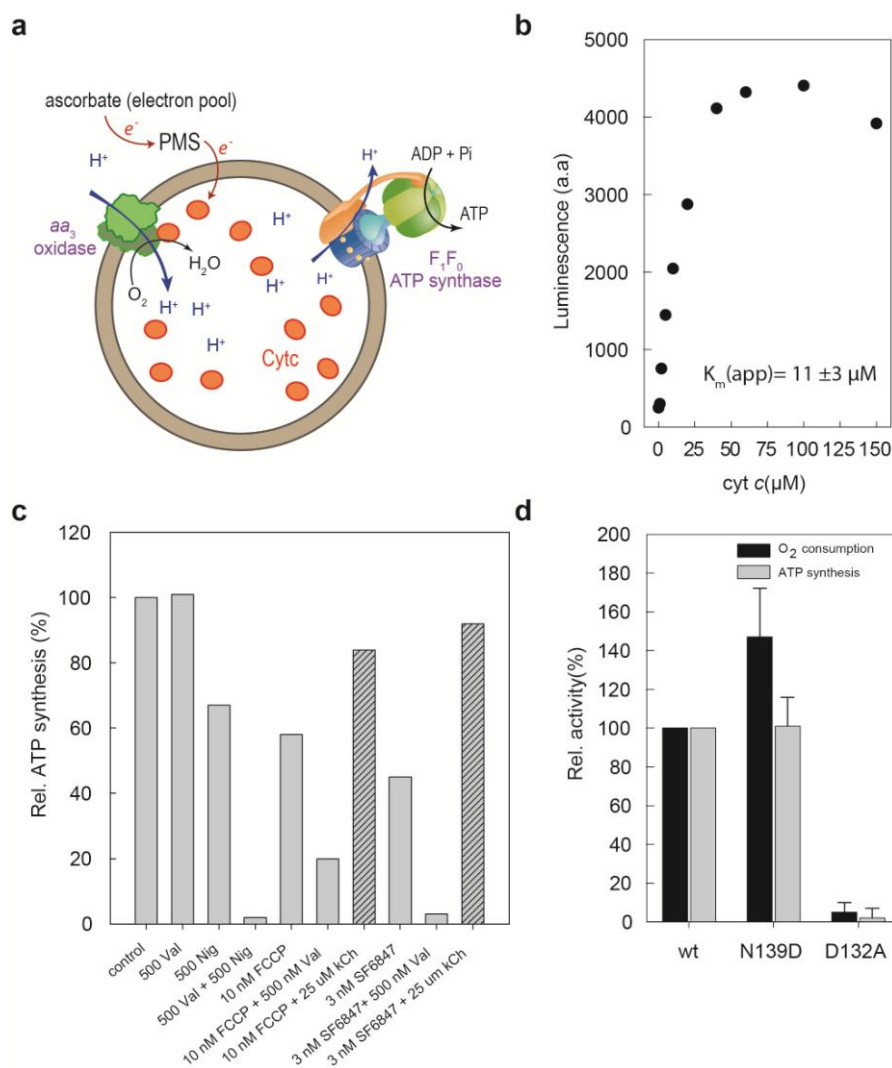


**Figure 4:** Respiratory driven ATP synthesis employing the  $aa_3$  oxidase from *R. sphaeroides* as proton pump.

(a) Cartoon showing proteoliposomes containing co-reconstituted ATP synthase and cytochrome *c* oxidase from *R. sphaeroides*, and incorporated cytochrome *c*. The electron donor ascorbate and electron mediator PMS are also indicated. Shown is the proton flux during ATP synthesis with correctly oriented enzymes. (b) Dependence of respiratory-driven ATP synthesis on the internal cytochrome *c* concentration, when 2 mM ascorbate and 10  $\mu M$  PMS were used as electron source and mediator, respectively. The indicated cyt *c* concentrations are those present in the reconstitution mixture prior to detergent removal. Shown is the result from a single experiment. The experiment was repeated two more times with fewer cyt *c* concentrations and similar results were obtained. An apparent  $K_m$  (average from three independent measurements) is given. (c) Inhibitor data as described in the text. See legend to Figure 3d for experimental details. Bars with a striped filling indicate the addition of 6-ketocholestenol. Shown are the results from a typical set of experiments. The measurements were performed with three different liposome preparations yielding similar results. (d) Comparison of oxygen turnover and respiratory-driven ATP synthesis for wild type and two structural variants of cytochrome *c* oxidase. Oxygen turnover (black bars) and respiratory-driven ATP synthesis (grey bars) were measured as described in the Materials and Methods section. The rates for the wild type enzyme were set to 100%. Shown are averaged values of two proteoliposome preparation measured in duplicate.

## Discussion

### General remarks

We present a facile and reproducible methodology for co-reconstitution of purified respiratory oxidases and ATP synthases from different organisms into preformed liposomes with a defined lipid composition and size. In the proteoliposomes, the oxidase builds up and maintains a transmembrane electrochemical gradient that is used by the  $F_1F_0$  ATP synthase to produce ATP, imitating the final steps of oxidative phosphorylation in mitochondria and many bacteria. The proteoliposomes exhibit continuous production of ATP on the outside of the liposomes, when supplied with ADP, phosphate, oxygen and a suitable electron donor/mediator couple to support proton pumping. In this regard, the proteoliposomes behave like submitochondrial particles or inverted bacterial membrane vesicles. However, in contrast to native membranes the protocol allows the variation of parameters such as the lipid composition, the protein-to-lipid ratio, liposome size, etc. In addition, structural variants of both enzymes can be investigated. Another advantage of the described system is the possibility to easily check for the effect of added compounds and the rather high time resolution of the measurements. In contrast to co-reconstituted bacteriorhodopsin/ATP synthase experiments, in which the sample is typically illuminated for tens of minutes, and synthesized ATP is measured discontinuously, we can immediately see the effect after the addition of a new compound.

### Protein orientation and protein-to-liposome ratio

A general complication associated with membrane protein reconstitution is that the enzyme orientation after incorporation cannot be strictly controlled. While some proteins show only a slight or no preference for one orientation, others seem to insert essentially unidirectionally [26, 28, 40, 41]. To our knowledge, no general strategy is known to solve this problem. In functional studies, this drawback can be circumvented in cases where a membrane-impermeable substrate is added, activating only the fraction of proteins with the substrate binding site oriented towards the outside (e.g. ATP with ATP synthase, cytochrome *c* with cytochrome *c* oxidase). In the case of a membrane-permeable substrate (e.g. ubiquinol for quinol oxidase), both populations are activated, and are expected to "compete" with each other.

The cholate/gel filtration method described in this manuscript has been shown to yield a unidirectional integration (> 95%) of the  $F_1F_0$  ATP synthase into liposomes, with the large soluble  $F_1$  part facing towards the outside [26]. The orientation of the ATP synthase is thus inverted compared to the situation found in bacteria or mitochondria, where the  $F_1$  headpiece is oriented towards the lumen (cytoplasm, mitochondrial matrix), but similar to that found in chloroplasts (facing the stroma). Consequently, in order to drive ATP synthesis in our system, protons have to be pumped to

the inside of the liposomes to create an electrochemical gradient that is positive and acidic on the inside. In the original work of Racker [15], bacterial ATP synthase was co-reconstituted with bacteriorhodopsin, and a bigger part of bacteriorhodopsin was inserted inside-out, i.e. it would acidify the inner lumen of liposomes upon illumination. Cytochrome *c* oxidases, however, tend to insert right way out (60-80%, [28]) with the soluble domain of subunit II (carrying the cytochrome *c* binding site) facing the outside of the liposomes. Proteins with this orientation, however, pump protons to the outside of the liposomes and are thus not suited for our purposes. Instead, the desired enzyme orientation (inside out) requires the presence of soluble cytochrome *c* and electrons on the inside of the liposome, requiring a membrane permeable electron mediator.

Using a different protocol, reconstitution of cytochrome *bo*<sub>3</sub> oxidase has been reported to insert preferably right way out, which is not surprising because of its similar molecular shape and subunit organization as cytochrome *c* oxidases [42]. As quinol oxidases take up electrons through the membrane via the water/membrane soluble ubiquinol Q<sub>1</sub>, both populations are expected to pump protons after addition of an electron source. So far, we have not been able to determine the *bo*<sub>3</sub> oxidase orientation in our proteoliposomes. However, our results from ACMA quenching experiments (Figure 1b) indicate that at least a fraction of liposomes shows a net proton influx, thus containing a majority of inside out oriented *bo*<sub>3</sub> oxidases. If the majority of enzymes are oriented right side out, increasing amounts of oxidase molecules per liposomes should decrease the relative number of liposomes with a “net proton influx”. However, we observed that increasing *bo*<sub>3</sub> concentrations (up to 30 enzymes per liposomes) further increased ATP production, not showing the expected effect of an inverted electrochemical potential (Supplementary Figure 5). This data implies one (or more) of the following explanations. First, our reconstitution method yields majorly inside out *bo*<sub>3</sub> oxidase orientation. Second, differential binding kinetics of ubiquinone Q<sub>1</sub> to the quinone site of the two enzyme populations could produce a kinetic asymmetry in enzyme turnover and thus proton transport. Third, localized proton transfer along the membrane surface [43-47] could lead to a rapid lateral distribution of pumped protons along the inner surface of the liposome (leading to significant local acidification and thus pH gradient). Clearly, more experiments are required to understand this process in more detail.

### **Electron supply for the terminal oxidases**

When the *bo*<sub>3</sub> oxidase from *E. coli* was utilized, electrons were supplied by DTT and mediated by ubiquinol Q<sub>1</sub> from the aqueous solution to the membrane embedded quinol binding site of *bo*<sub>3</sub> oxidase. In addition, we also obtained ATP synthesis using NADH and human DT-Diaphorase that is able to reduce short-chained quinones (like Q<sub>1</sub>) in aqueous solutions [48].

Electron supply to the inside of the liposomes, as it is necessary for the  $aa_3$  cytochrome *c* oxidase, is more difficult to accomplish. As outlined in the Results section, we tried several combinations of electron donor and mediator couples and found ascorbate (2 mM) and PMS (10  $\mu$ M with 15  $\mu$ M cytochrome *c*) to be the most suitable electron donor-mediator couple. PMS in its oxidized form is a positively charged membrane-permeable molecule which is able to keep its hydrophobicity in the charged state by charge delocalization through the conjugated aromatic ring system. In our experiments, we therefore envision the following scenario: The membrane impermeable ascorbate reduces PMS on the outside to its semi-reduced or reduced form (neutral), which freely passes the membrane to deliver electrons to cytochrome *c* on the inside of the vesicles [49]. The passage of reduced PMS across the membrane is thus electroneutral (otherwise it would not occur in the first place) and will not impose a counteracting membrane potential. After delivery of its electron to cytochrome *c* and release of a proton, the oxidized PMS (positively charged) leaves the liposome driven by the membrane potential (created by the cytochrome *c* oxidase) to receive another electron from ascorbate and pick up a proton. PMS transport out of the liposomes is (probably) electrogenic and decreases the total proton driving force slightly. Furthermore, in the presence of excess of ascorbate, PMS in micromolar concentrations is also capable of directly reducing oxygen, competing with cytochrome *c* oxidase and luciferase for oxygen. Consequently, measurement times with  $aa_3$  oxidase in the presence of 10  $\mu$ M PMS were considerably shorter (2 minutes) than with  $bo_3$  oxidase. Using lower amounts of PMS, e.g. 2  $\mu$ M, extends measuring time to >5min, but also decreased the ATP synthesis rate by a factor of  $\sim 2$ . Furthermore, PMS seems to have an effect as an uncoupler of the membrane potential and thus decreased the apparent  $IC_{50}$  of ionophores (Supplementary Figure 4). For these reasons, we generally preferred the  $bo_3$ /ATP synthase over the  $aa_3$ /ATP synthase system in our studies.

### Estimation of ATP synthase turnover rate

The reported turnover rates of ATP synthases from purified components differ significantly between organisms (and laboratories), as measurements were done under different conditions and a direct comparison is not straightforward. The highest rates (up to 300 ATP  $\times$   $s^{-1}$   $\times$  enzyme $^{-1}$ ) have been measured with the chloroplast enzyme, while the *E. coli* ATP synthase was >4 times slower under the same very high energizing conditions ( $\Delta pH + \Delta \psi > 360$  mV) [50]. In inverted membrane vesicles of *E. coli* (a system that is probably most related to our system), rates of  $\sim 30$  ATP  $\times$   $s^{-1}$   $\times$  enzyme $^{-1}$  were measured at 25°C when the membranes were energized with NADH via respiratory complex I. The turnover rate was increased to  $\sim 250$  ATP  $\times$   $s^{-1}$   $\times$  enzyme $^{-1}$ , when 95% of the ATP synthases were inhibited and the temperature was increased to 37°C. In proteoliposomes with the purified enzyme from *E. coli*, rates up to 75 ATP  $\times$   $s^{-1}$   $\times$  enzyme $^{-1}$  have been reported, when a very large driving force was applied (pH gradient >4 pH units and a  $\Delta \psi$  of  $\sim 120$  mV, total driving force of >360 mV) [50]. A

disadvantage of this type of measurements is the requirement of a potassium/valinomycin diffusion potential that exhausts very quickly, i.e. the measuring time is limited to a few seconds and the turnover numbers are calculated from initial rates.

We also estimated the ATP synthase turnover rate in our co-reconstituted system. Assuming a reconstitution efficiency of 50% [27], liposomes containing 10  $bo_3$  oxidases and 3 ATP synthases were used. With this preparation, we observed turnover rates of up to 90 ATP  $\times$  s<sup>-1</sup>  $\times$  enzyme<sup>-1</sup> at 25°C, which is similar to those reported for the *in vitro* systems discussed above (a typical calculation is exemplified in the supplementary data). A reliable calculation depends on many factors (enzyme purity and integrity, reconstitution efficiency) and we are thus careful to not over interpret these calculations. A further critical factor is the fraction of active liposomes (see discussion of  $bo_3$  oxidase orientation above), as any ATP synthase in an inactive liposome will not contribute to ATP synthesis. Nonetheless, our estimated rates are significantly higher than those measured using bacteriorhodopsin as a proton pump (c.f.  $\sim$ 6 ATP  $\times$  s<sup>-1</sup>  $\times$  enzyme<sup>-1</sup>) [17], suggesting that the  $bo_3$  oxidase creates a larger electrochemical gradient than bacteriorhodopsin. For the ATP synthase from spinach chloroplasts, we obtained rates of 50 - 80 ATP  $\times$  s<sup>-1</sup>  $\times$  enzyme<sup>-1</sup>, assuming an 80% purity of the preparation. While these rates are lower than those measured with the isolated enzyme with a very high driving force [50], it is markedly faster than the comparable experiment with bacteriorhodopsin ( $\sim$ 9 ATP  $\times$  s<sup>-1</sup>  $\times$  enzyme<sup>-1</sup>) [51], supporting our findings with the  $bo_3$  oxidase.

### Equivalence of driving forces

ATP synthesis by the ATP synthase is energized by the proton motive force consisting of a chemical proton gradient and the membrane potential. Additionally, for the *E. coli* enzyme it has been reported that the pH at *p*-side (proton entry side) has to be below pH 6.5 to allow efficient ATP synthesis, while almost no ATP synthesis was observed above pH 7 under otherwise identical driving forces [31]. While both components are thermodynamically identical, the kinetic equivalence in ATP synthesis is debated and has not been observed in all organisms [26, 31, 50, 52]. The use of ionophores in our minimal system to specifically abolish either of the two components offers thus a valuable tool to investigate the functional characteristics of the ATP synthase. The individual effect of these ionophores could not be investigated in earlier *in vitro* experiments, as the potassium-specific ionophore valinomycin is required to establish the electrical component of the proton-motive force. It is noteworthy that in our experiments, addition of NH<sub>4</sub>Cl (in the absence of valinomycin) prevented the buildup of a transmembrane proton gradient, as confirmed by ACMA quenching, but it did barely affect the ATP synthesis rate (see **Figure 3a**). A possible explanation is that the lacking chemical gradient was compensated by a larger membrane potential. However, in the presence of NH<sub>4</sub>Cl, the *p*-side pH would be identical to the pH (7.5) of the measuring buffer, which is well above the minimal

requirements found for the ATP synthase [31]. It has thus been proposed that upon proton pumping, local acidification at the membrane surface could provide the required low pH at the *p*-side of the enzyme [31]. Interestingly, this low pH requirement is absent in proton-translocating experiments with only the  $F_0$  part of the *E. coli* ATP synthase, where  $\Delta\psi$  and  $\Delta\text{pH}$  were equivalent driving forces [26]. On the other hand, no *in vitro* measurements with the *E. coli* enzyme have been reported, where ATP synthesis is solely driven by a  $\Delta\psi$ . Recently, however, ATP synthesis exclusively driven with a  $\Delta\psi$  has been demonstrated for the ATP synthase from *Bacillus PS3* lacking part of subunit  $\epsilon$  (in presence of the intact  $\epsilon$  subunit, ATP synthesis is 20-times lower) [52]. More experiments are required to understand the fundamental nature of driving ATP synthesis.

### **Mild uncoupling and recoupling of respiratory phosphorylation**

After addition of the proton ionophore FCCP at concentrations  $<200$  nM, notable synthesis of ATP was still observed. FCCP is well known as a strong uncoupling agent of respiratory phosphorylation in mitochondria, but low dosages of FCCP ( $<100$  nM) have been shown to primarily affect the respiratory-control ratio, but not ATP synthesis, a phenomenon termed “mild uncoupling” [53, 54]. We were able to reproduce this behavior using our experimental system with similar FCCP concentrations. Accordingly, we did also observe the recoupling effect of 6-ketocholestanol [34, 35, 53]. As in mitochondria, recoupling at fully uncoupling concentrations of FCCP was not observed. The original data were interpreted to indicate that “mild uncoupling” could involve a specific protein binding site for compounds similar to FCCP and SF6748 in the inner mitochondrial membrane [54], and results from experiments with proteoliposomes containing purified mitochondrial cytochrome *c* oxidase suggested that this protein was the main target [54]. Our data, however, indicate that the phenomenon is more likely an effect of the intrinsic properties of the membrane. Firstly, only bacterial proteins were utilized in our experiments, excluding the possibility of a specific mitochondrial property. Secondly, proteoliposomes containing either  $aa_3$  oxidase or  $bo_3$  oxidase as primary proton pump show a similar effect of uncoupling and recoupling, making a specific cytochrome *c* oxidase effect unlikely. The originally proposed underlying mechanism for the recoupling effect is that 6-ketocholestanol mainly inserts in the outer leaflet of the membrane thus creating an asymmetry and a membrane dipole potential. The asymmetric insertion (and slowed leaflet flipping) is favored by the additional keto group that increases the polarity and thus the amphiphilic character of the cholesterol derivative. This asymmetric insertion was suggested to hinder binding of FCCP and other uncoupling agents to their protein target. Our data suggest that a protein is not likely involved in this process. Instead, such a dipole potential could interfere with the electrogenic diffusion of the anionic form of the uncoupler. Such interference could slow the



“recycling” of the catalytically active uncoupler to the acidic side of the membrane, thereby slowing the overall uncoupling process.

No change in the ATP-synthesis rate was observed upon addition of the potassium-specific ionophore valinomycin at concentrations that are well above the ones required to build up or dissipate a membrane potential (20-200 nM) in the presence of potassium [26]. As valinomycin dissipates the electrical potential, the oxidase turnover activity is expected to increase, thereby increasing the proton concentration gradient. In other words, in the presence of valinomycin the membrane electrical potential is converted into a proton concentration gradient. In contrast to  $\Delta\psi$ ,  $\Delta\text{pH}$  alone has been shown to successfully drive ATP synthesis with the *E. coli* enzyme [31, 50] and accordingly, no significant change is observed in the ATP synthesis rate. However, if valinomycin is combined with proton gradient dissipating molecules such as Nigericin, FCCP or SF6847 or  $\text{NH}_4\text{Cl}$ , also the proton gradient is dissipated and no ATP synthesis is observed (**Figure 3c and 4d**). An enhanced sensitivity towards uncouplers in the presence of valinomycin was also described for mitochondria and chloroplasts [55].

The same argumentation can also be used to explain the behavior of the N139D variant of the  $\alpha\alpha_3$  cytochrome *c* oxidase, which is disabled in proton pumping yet showing a similar ATP synthesis activity to that of the wild-type oxidase. In cytochrome *c* oxidase, electrons are donated from cytochrome *c* from the positive side of the membrane, while protons used for reduction of oxygen are taken from the negative side of the membrane. Furthermore, the electron transfer from PMS to cytochrome *c* is accompanied by a release of protons to the inside of the liposomes. In other words, even in the absence of proton pumping, an electrochemical gradient ( $\Delta\text{pH}$  and  $\Delta\psi$ ) is generated by the oxidase, although with an efficiency of 50 % compared to that obtained with the wild-type oxidase (separation of one charge instead of two, across the membrane for each electron transferred to oxygen). With the N139D structural variant, the same transmembrane electrochemical potential would be maintained as with the wild-type oxidase, but at a twice higher turnover rate. The D139N variant has indeed an already higher turnover activity than the wild type oxidase in detergent solution and the difference between the two is expected to further increase in membranes because of the reasons discussed above, i. e. a lower membrane potential allows a larger proton gradient.

## Concluding remarks

The described experimental system allows the control of many experimental parameters and the requirement of small amounts of protein ( $\sim 40 \mu\text{g}$  *bo*<sub>3</sub> oxidase per reconstitution or  $\sim 1 \mu\text{g}$  per

measurement were used) what makes it an attractive tool for the investigation of energetically coupled processes in the membrane. The novel experimental system was used to investigate the phenomenon of "mild uncoupling", which has been suggested to prevent ROS formation under low phosphorylation activity in mitochondria, and has therefore attracted some interest [8, 12-14]. While some uncoupling processes are clearly protein mediated (e.g. UCP 1), others, such as those using low concentrations of uncoupling compounds are not well understood. Our simple experimental setup with only two proteins (i.e. excluding protein mediated uncoupling pathways via UCPs and/or the ADP/ATP translocase) mimics the behavior found in mitochondria very well and allowed us to exclude direct uncoupler-protein interactions as a possible explanation for mild uncoupling.

### **Acknowledgements**

We thank Pia Ädelroth for valuable discussions. The work was supported by the Swiss National Science Foundation (SNFS), the Swedish Research Council (VR) and the Knut and Alice Wallenberg Foundation (KAW).

## References

- [1] M. Saraste, Oxidative phosphorylation at the *fin de siecle*, *Science*, 283 (1999) 1488-1493.
- [2] P.R. Rich, A. Marechal, The mitochondrial respiratory chain, *Essays Biochem*, 47 (2010) 1-23.
- [3] P.D. Boyer, The ATP synthase- a splendid molecular machine, *Annu. Rev. Biochem.*, 66 (1997) 717-749.
- [4] C. von Ballmoos, G.M. Cook, P. Dimroth, Unique Rotary ATP Synthase and Its Biological Diversity, *Ann Rev Biophys*, 37 (2008) 43-64.
- [5] C. von Ballmoos, A. Wiedenmann, P. Dimroth, Essentials for ATP synthesis by  $F_1F_0$  ATP synthases, *Ann Rev Biochem*, 78 (2009) 649-672.
- [6] V.P. Skulachev, Role of uncoupled and non-coupled oxidations in maintenance of safely low levels of oxygen and its one-electron reductants, *Quarterly Reviews of Biophysics*, 29 (1996) 169-202.
- [7] J.A. Sanchez-Alcazar, J.G. Ault, A. Khodjakov, E. Schneider, Increased mitochondrial cytochrome c levels and mitochondrial hyperpolarization precede camptothecin-induced apoptosis in Jurkat cells, *Cell Death Differ*, 7 (2000) 1090-1100.
- [8] M.D. Brand, J.A. Buckingham, T.C. Esteves, K. Green, A.J. Lambert, S. Miwa, M.P. Murphy, J.L. Pakay, D.A. Talbot, K.S. Echtay, Mitochondrial superoxide and aging: Uncoupling-protein activity and superoxide production, in: *Biochemical Society Symposium*, 2004, pp. 203-213.
- [9] A. Perl, G. Nagy, P. Gergely, F. Puskas, Y. Qian, K. Banki, Apoptosis and mitochondrial dysfunction in lymphocytes of patients with systemic lupus erythematosus, *Methods Mol Med*, 102 (2004) 87-114.
- [10] V.P. Skulachev, Bioenergetic aspects of apoptosis, necrosis and mitoptosis, *Apoptosis*, 11 (2006) 473-485.
- [11] B. Cannon, I.G. Shabalina, T.V. Kramarova, N. Petrovic, J. Nedergaard, Uncoupling proteins: A role in protection against reactive oxygen species - or not?, *Bba-Bioenergetics*, 1757 (2006) 449-458.
- [12] K.S. Echtay, D. Rousset, J. St-Pierre, M.B. Jekabsons, S. Cadenas, J.A. Stuart, J.A. Harper, S.J. Roebuck, A. Morrison, S. Pickering, J.C. Clapham, M.D. Brand, Superoxide activates mitochondrial uncoupling proteins, *Nature*, 415 (2002) 96-99.
- [13] B. Kadenbach, Intrinsic and extrinsic uncoupling of oxidative phosphorylation, *Bba-Bioenergetics*, 1604 (2003) 77-94.
- [14] P.S. Brookes, Mitochondrial H + leak and ROS generation: An odd couple, *Free Radical Biology and Medicine*, 38 (2005) 12-23.
- [15] E. Racker, W. Stoeckenius, Reconstitution of purple membrane vesicles catalyzing light-driven proton uptake and adenosine triphosphate formation, *J Biol Chem*, 249 (1974) 662-663.
- [16] B. Pitard, P. Richard, M. Dunach, G. Girault, J.L. Rigaud, ATP synthesis by the FOF1 ATP synthase from thermophilic *Bacillus PS3* reconstituted into liposomes with bacteriorhodopsin. 1. Factors defining the optimal reconstitution of ATP synthases with bacteriorhodopsin, *Eur J Biochem*, 235 (1996) 769-778.
- [17] B. Pitard, P. Richard, M. Dunach, J.L. Rigaud, ATP synthesis by the FOF1 ATP synthase from thermophilic *Bacillus PS3* reconstituted into liposomes with bacteriorhodopsin. 2. Relationships between proton motive force and ATP synthesis, *Eur J Biochem*, 235 (1996) 779-788.
- [18] C. Etzold, G. Deckers-Hebestreit, K. Altendorf, Turnover number of *Escherichia coli*  $F_0F_1$  ATP synthase for ATP synthesis in membrane vesicles, *Eur. J. Biochem.*, 243 (1997) 336-343.

- [19] T. Vorburger, J. Zingg Ebnetter, A. Wiedenmann, D. Morger, G. Weber, K. Diederichs, P. Dimroth, C. von Ballmoos, Arginine-induced conformational change in the c-ring/a-subunit interface of ATP synthase, *Febs J*, 275 (2008) 2137-2150.
- [20] P. Turina, D. Samoray, P. Gräber, H<sup>+</sup>/ATP ratio of proton transport-coupled ATP synthesis and hydrolysis catalysed by CF<sub>0</sub>F<sub>1</sub>-liposomes, *EMBO J.*, 22 (2003) 418-426.
- [21] H.L. Frericks, D.H. Zhou, L.L. Yap, R.B. Gennis, C.M. Rienstra, Magic-angle spinning solid-state NMR of a 144 kDa membrane protein complex: *E. coli* cytochrome *bo*<sub>3</sub> oxidase, *J Biomolecular NMR*, 36 (2006) 55-71.
- [22] D.M. Mitchell, R.B. Gennis, Rapid purification of wildtype and mutant cytochrome *c* oxidase from *Rhodobacter sphaeroides* by Ni(2+)-NTA affinity chromatography, *FEBS letters*, 368 (1995) 148-150.
- [23] P.S. Chen, Jr., T.Y. Toribara, H. Warner, Microdetermination of phosphorus, *Anal. Chem.*, 28 (1956) 1756-1758.
- [24] J.L. Rigaud, B. Pitard, D. Levy, Reconstitution of membrane proteins into liposomes: application to energy-transducing membrane proteins, *Biochim. Biophys. Acta*, 1231 (1995) 223-246.
- [25] R.R. Ishmukhametov, M.A. Galkin, S.B. Vik, Ultrafast purification and reconstitution of His-tagged cysteine-less *Escherichia coli* F<sub>1</sub>F<sub>0</sub> ATP synthase, *Biochim. Biophys. Acta*, 1706 (2005) 110-116.
- [26] A. Wiedenmann, P. Dimroth, C. von Ballmoos, Dy and DpH are equivalent driving forces for proton transport through isolated F<sub>0</sub> complexes of ATP synthases, *Biochim Biophys Acta*, 1777 (2008) 1301-1310.
- [27] G. Nordlund, P. Brzezinski, C. von Ballmoos, SNARE-fusion mediated insertion of membrane proteins into native and artificial membranes, *Nature communications*, 5 (2014) 4303.
- [28] L. Näsvisk Öjemyr, C. von Ballmoos, K. Faxen, E. Svahn, P. Brzezinski, The membrane modulates internal proton transfer in cytochrome *c* oxidase, *Biochemistry*, 51 (2012) 1092-1100.
- [29] H.I. Petrache, S.W. Dodd, M.F. Brown, Area per Lipid and Acyl Length Distributions in Fluid Phosphatidylcholines Determined by 2H NMR Spectroscopy, *Biophys J*, 79 (2000) 3172-3192.
- [30] S. Fischer, C. Etzold, P. Turina, G. Deckers-Hebestreit, K. Altendorf, P. Gräber, ATP synthesis catalyzed by the ATP synthase of *Escherichia coli* reconstituted into liposomes, *Eur. J. Biochem.*, 225 (1994) 167-172.
- [31] A. Wiedenmann, P. Dimroth, C. von Ballmoos, Functional asymmetry of the F<sub>0</sub> motor in bacterial ATP synthases, *Mol Microbiol*, 72 (2009) 479-490.
- [32] P. Richard, B. Pitard, J.L. Rigaud, ATP synthesis by the F<sub>0</sub>F<sub>1</sub>-ATPase from the thermophilic *Bacillus PS3* co-reconstituted with bacteriorhodopsin into liposomes. Evidence for stimulation of ATP synthesis by ATP bound to a noncatalytic binding site, *J Biol Chem*, 270 (1995) 21571-21578.
- [33] R. Benz, S. McLaughlin, The molecular mechanism of action of the proton ionophore FCCP (carbonylcyanide *p*-trifluoromethoxyphenylhydrazone), *Biophys J*, 41 (1983) 381-398.
- [34] A.A. Starkov, D.A. Bloch, B.V. Chernyak, V.I. Dedukhova, S.E. Mansurova, I.I. Severina, R.A. Simonyan, T.V. Vygodina, V.P. Skulachev, 6-ketocholestanol is a recoupler for mitochondria, chromatophores and cytochrome oxidase proteoliposomes, *Bba-Bioenergetics*, 1318 (1997) 159-172.
- [35] A.A. Starkov, V.I. Dedukhova, V.P. Skulachev, 6-Ketocholestanol Abolishes the Effect of the Most Potent Uncouplers of Oxidative-Phosphorylation in Mitochondria, *Febs Letters*, 355 (1994) 305-308.
- [36] S. Ferguson-Miller, C. Hiser, J. Liu, Gating and regulation of the cytochrome *c* oxidase proton pump, *Bba-Bioenergetics*, 1817 (2012) 489-494.
- [37] P. Brzezinski, P. Adelroth, Design principles of proton-pumping haem-copper oxidases, *Curr Opin Struc Biol*, 16 (2006) 465-472.
- [38] A.S. Pawate, J. Morgan, A. Namslauer, D. Mills, P. Brzezinski, S. Ferguson-Miller, R.B. Gennis, A mutation in subunit I of cytochrome oxidase from *Rhodobacter sphaeroides* results in an increase in

steady-state activity but completely eliminates proton pumping, *Biochemistry*, 41 (2002) 13417-13423.

[39] J.R. Fetter, J. Qian, J. Shapleigh, J.W. Thomas, A. GarciaHorsman, E. Schmidt, J. Hosler, G.T. Babcock, R.B. Gennis, S. Fergusonmiller, Possible Proton Relay Pathways in Cytochrome-C-Oxidase, *P Natl Acad Sci USA*, 92 (1995) 1604-1608.

[40] M. Seigneuret, J.L. Rigaud, Partial Separation of Inwardly Pumping and Outwardly Pumping Bacteriorhodopsin Reconstituted Liposomes by Gel-Filtration, *FEBS Letters*, 228 (1988) 79-84.

[41] J. Knol, L. Veenhoff, W.J. Liang, P.J. Henderson, G. Leblanc, B. Poolman, Unidirectional reconstitution into detergent-destabilized liposomes of the purified lactose transport system of *Streptococcus thermophilus*, *J. Biol. Chem.*, 271 (1996) 15358-15366.

[42] M.L. Verkhovskaya, A. GarciaHorsman, A. Puustinen, J.L. Rigaud, J.E. Morgan, M.I. Verkhovsky, M. Wikstrom, Glutamic acid 286 in subunit I of cytochrome bo(3) is involved in proton translocation, *P Natl Acad Sci USA*, 94 (1997) 10128-10131.

[43] R.J. Williams, The multifarious couplings of energy transduction, *Biochim. Biophys. Acta*, 505 (1978) 1-44.

[44] A.Y. Mulkidjanian, J. Heberle, D.A. Cherepanov, Protons @ interfaces: implications for biological energy conversion, *Biochim. Biophys. Acta*, 1757 (2006) 913-930.

[45] J. Heberle, J. Riesle, G. Thiedemann, D. Oesterhelt, N.A. Dencher, Proton migration along the membrane surface and retarded surface to bulk transfer, *Nature*, 370 (1994) 379-382.

[46] P. Ädelroth, P. Brzezinski, Surface-mediated proton-transfer reactions in membrane-bound proteins, *Biochim Biophys Acta*, 1655 (2004) 102-115.

[47] M. Branden, T. Sanden, P. Brzezinski, J. Widengren, Localized proton microcircuits at the biological membrane-water interface, *Proc Natl Acad Sci U S A*, 103 (2006) 19766-19770.

[48] R.E. Beyer, J. Segura-Aguilar, S. Di Bernardo, M. Cavazzoni, R. Fato, D. Fiorentini, M.C. Galli, M. Setti, L. Landi, G. Lenaz, The role of DT-diaphorase in the maintenance of the reduced antioxidant form of coenzyme Q in membrane systems, *Proc Natl Acad Sci U S A*, 93 (1996) 2528-2532.

[49] W.S. Zaugg, A. Tirpack, L.P. Vernon, Photoreduction of Ubiquinone + Photooxidation of Phenazine Methosulfate by Chromatophores of Photosynthetic Bacteria + Bacteriochlorophyll, *P Natl Acad Sci USA*, 51 (1964) 232-&.

[50] S. Fischer, P. Gräber, Comparison of DeltapH- and Deltay-driven ATP synthesis catalyzed by the H<sup>+</sup>-ATPases from *Escherichia coli* or chloroplasts reconstituted into liposomes, *FEBS Lett.*, 457 (1999) 327-332.

[51] J. Krupinski, G.G. Hammes, Steady-state ATP synthesis by bacteriorhodopsin and chloroplast coupling factor co-reconstituted into asolectin vesicles, *Proc Natl Acad Sci U S A*, 83 (1986) 4233-4237.

[52] N. Soga, K. Kinoshita, Jr., M. Yoshida, T. Suzuki, Kinetic equivalence of transmembrane pH and electrical potential differences in ATP synthesis, *J Biol Chem*, 287 (2012) 9633-9639.

[53] V.P. Skulachev, Uncoupling: new approaches to an old problem of bioenergetics, *Biochim Biophys Acta*, 1363 (1998) 100-124.

[54] A.A. Starkov, "Mild" uncoupling of mitochondria, *Biosci Rep*, 17 (1997) 273-279.

[55] S.J.D. Karlish, N. Shavit, M. Avron, On Mechanism of Uncoupling in Chloroplasts by Ion-Permeability Inducing Agents, *European Journal of Biochemistry*, 9 (1969) 291-&.

Von Ballmoos et al:

Highlights:

- The functional co-reconstitution of terminal oxidases and ATP synthase is described
- The experimental setup is used with enzymes from different organisms
- Steady state ATP synthesis at high rates are observed
- Mild uncoupling is not a protein dependent process

ACCEPTED MANUSCRIPT